Journal of Robotics and Control (JRC)
Volume 6, Issue 2, 2025
ISSN: 2715-5072, DOI: 10.18196/jrc.v6i2.24599

Novel Hybrid SM Strategy Based on Speed Control and Disturbances Rejection for High Performance DSIM Drives

Ngoc Thuy Pham [1*]
[1] Dept. of Electrical Engineering Technology, Industrial University of Ho Chi Minh City, Viet Nam
Email: [1] ngocpham1020@gmail.com
*Corresponding Author

***Abstract*—In control theory and applications, disturbance cancellation is a critical challenge in the control of nonlinear drive systems, particularly in applications involving Dual Star Induction Motors (DSIM). This paper proposes a new adaptive hybrid sliding mode (SM) strategy that integrates a Repetitive Control (RC) scheme into an improved Second-Order Sliding Mode (SOSM) structure. The goal is to enhance tracking accuracy and periodic harmonic disturbance rejection in DSIM drive systems. The strategy also incorporates a load torque disturbance estimator that efficiently identifies and cancels disturbances, further improving system performance. System stability is guaranteed using Lyapunov theory, ensuring that the virtual control vectors for speed and current loops maintain stability throughout the operation. Simulation results using MATLAB confirm the effectiveness of the proposed control strategy, demonstrating improved tracking performance, harmonic disturbance rejection, and robust operation of the DSIM under varying conditions.**

Keywords—Variable Gain Super Twisting Algorithm; Second Order Sliding Mode; Dual Start Induction Motor; FOC; Vector Control; Repetitive Control; Disturbance Cancellation.

I. INTRODUCTION

The DSIM drives are one of the multiphase motor drives received very much attention, it has been focused on research in recent decades and applied in the high-power industrial applications, in the systems that requires high quality control, the reliability and capability high fault tolerance. Especially, they applied for the drives in transportation field such as electric vehicles (EV), ship, aeronautics, ... Today, with the outstanding advantages, DSIM also is replaced three-phase induction motors in traditional three-phase AC drives that require high reliability, accuracy, safety and fault tolerance [1]-[7]. However, DSIM has its inherent problems of nonlinearity and coupling, which are challenges for control systems design. Additionally, the external disturbances such as suddenly load changes, periodic disturbances also decreases the performance of the drives.

The good control of loops is the key to achieving high performance for SPIM drives. However, various disturbances appearing during the control process always negatively affect the performance of the loops, so many control methods have been focused on research to meet the requirements of accurate tracking and strong harmonic rejection [8]-[9].

Now, the control methods have been developed based on modern vector control strategies for DSIM drives. In that, Direct torque control (DTC) first introduced by Takahashi in the mid-1980s, has proven to be highly successful with the concept of reducing dependence on the parameters of motor inductance and increasing the accuracy and dynamics of magnetic flux and torque response. This is a simple control strategy, the advantages of DTC are giving the fast response and less dependence on machine parameter changes, it also does not require any transformation of coordinates or current control loops, so it is quite simple. However, DTC faces major disadvantages that are high switching frequency, torque and flux ripples, mechanical vibration and noise of the machine, poor control performance when operating in low-speed ranges [10]-[17]. In opposition to DTC, the Field Oriented Control (FOC) has been developed in the early 1970s, which includes two techniques, that are the Direct Field Oriented Control (DFOC), proposed by Blaschke in 1972, and indirect Field Oriented Control (IFOC), proposed by Hasse in 1968. Theoretically, FOC based on Fleming's law gives the control performance of IM as good as that of DC motors, where the torque and flux are decoupled and can therefore be controlled independently. This control method gives fast torque response, a wide speed control range and high efficiency over a wide load variation range. The problems such as flux and torque ripples, noise and mechanical vibration of the motor, poor control performance at low speeds have not appeared in FOC control. However, besides the outstanding advantages mentioned above, the disadvantages of FOC are the performance of this control strategy affected by factors such as control model and motor parameters and has a great complexity caused by the presence of coordinate transformations and the use of several control variables, so when applying the PI control method for traditional FOC with fixed coefficients, it does not meet the quality of control for high-performance drives [18]-[23].

The modern and intelligent controls are proposed to deal these problems [24]-[40]. Among, the sliding mode (SM) control one of the most outstanding methods, it has been widely employed in many industrial applications due to its robustness against internal and external disturbances, simple, easy tuning and implementation [25]-[31]. However, there are two main restrictions remain. First, the constraint to be held at zero in conventional sliding modes has to be of relative degree 1, which means that the control needs to explicitly appear in the first time derivative of the constraint. Thus, one has to search for an appropriate constraint. Second, high-frequency control switching may easily cause unacceptable practical complications (chattering effect), if the control has any physical sense. Several methods were proposed to eliminate this unwanted phenomenon such as the use of the discontinuous sign function, SOSM or high-order SM control [29]-[30], ... In that, the second order sliding control allows to eliminate or to reduce the chattering phenomenon. Its main purpose is to generate a second order sliding mode on a selected sliding surface S(t, x). Unlike SOSM or the standard twisting algorithm, this supper twisting algorithm is only able to stabilize in finite time systems whose relative degree is equal to one and then it does not require information about the time derivative of the sliding variable help improve more performance of SOSM. The variable-gain super twisting algorithm (VGSTA) continues the extension of the standard super-twisting algorithm for the conventional SOSM controller design proccess. VSTASOSM provides exact compensation of uncertainties/disturbances bounded together with their derivatives by known functions and this algorithm also is considered as a discrete version of sliding mode control (DSM), it has not the same properties as the continuous SM because of the finite sampling rate. When referring to DSM, its sensitivity to parameter uncertainties, nonlinearities and external disturbances are the main problems that affect to performance of this controller.

Up today, many research were developed for DSM but these studies are mainly based on the assumption that nonlinear systems are affected only by habitual disturbances, however, in fact, in a variety of nonlinear industrial processes (mechanical, robotics, power distribution, etc.) are disturbances can be harmonic signals, the diode rectifiers, power converters,... can be considered as a generator of these non-desired harmonic currents [41], Cogging torque, that caused by the misalignment between stator and rotor is the important periodic disturbances affect rotating mechanical machines [42]. Or the periodic disturbances that appears due to the eccentricity of the track in the hard disk drives [43], due to the interaction between rigid hub and fexible appendage during attitude manoeuvrer in spacecraft [44]. Therefore, the major challenge of nonlinear drive system where existing periodic disturbances is the design of an accurate control ensuring good tracking and rejecting disturbance performances.

The harmonic disturbance cancellation is great importance in the control applications. In fact, it is easy to see that, in a drive systems, if both the precise mathematical model and harmonic disturbance frequency are known, the disturbance the compensate will use the feedback techniques based on internal model principles in [45], In the case, if just the precise system model of the system is known, a disturbance observer to reconstruct harmonic disturbance is designed, as shown in [46]. On the other hand, if a mathematical model is not available, the adaptive control techniques can be developed as in [47]. In the case, unknown harmonic disturbances and uncertain system models the feedforward techniques is applied as in [48]. Adaptive control methods based on feedback can also be proposed to tackle known and unknown disturbance frequencies [49]-[50]. They, however, generally require some extra information and structural assumptions regarding the system. The presence of harmonic disturbance in the system can also be seen, described, and eventually resolved in the framework of active disturbance rejection control, or ADRC. In this technique, all the uncertain elements called total disturbance of the system, seen from the plant perspective as an input-additive. The main concept of ADRC is that a detailed analytical representation of the system is not required for control synthesis as long as the influence of aggregated disturbance on the controlled output is continuously mitigated. Such output invariance, thus trivialization of the control design, can be achieved through on-line reconstruction of the total disturbance by means of a specialized observer. The interest in the ADRC idea also comes from its practical appeal, verified to date in numerous power motion and process applications [50]-[51]. For those reasons, the ADRC approach has been previously applied to the problem of harmonic disturbance compensation, with examples being and most recently [52]. Combining these disturbance rejection strategies with disturbance observers and compensation is required to give the good disturbance cancellation efficiency but these making control system more complex [53].

In contrary to the above solutions, [54] develops a unique disturbance rejection scheme for highly uncertain systems subjected to harmonic disturbances with unknown/known frequencies. Repetitive control (RC) was proved to be an effective tool to reject disturbance and enhance the control performance by its repeated learning process. However, it faces the stability problem and the inability to consider certain characteristics of processes [54]-[55]. To overcome these, many research focus on improve the RC design for non-linear systems [56]-[58]. Especially, modified RC based on disturbance observer (MRC) was developed in to ensure the high-frequency stability and low-frequency periodic disturbances resist ability of the control strategy, a robust plug-in RC with phase compensation was proposed in [56]. Another approach that the combination of RC with SM, an IIR low-pass filter was applied inside the internal model of RC to improve the stability robustness, is developed in [57]. In [58], a multi-model identification in presence of the periodic disturbance with adaptive filter is used to decouple the disturbance and a discrete repetitive sliding mode multi-control are developed are developed to deal the problem of stability of the systems, the proposed control technique in [58] also combined multi-model SM control with RC to enhance the control performances of nonlinear systems.

In this paper, to thoroughly solve the problems of periodic harmonic disturbance and accurately track for high performance DSIM drives, a new improved sliding mode control method is proposed.

The main contributions are summarized as follows:

– The improved sliding mode control technique is developed by embedding the variable-gain super twisting algorithm to exact compensation of uncertainties/ disturbances into the improved second order sliding mode control to improve the large control effort and reject the chattering phenomena.

– Repetitive Control is also integrated into this improved VGSTASOSM structure, combining of the benefits of improved SOSM with RC helps effectively improve FOC vector control performances in terms of tracking and rejection of harmonic disturbance for DSIM drives.

The rest paper part is structured is being as: The mathematical model of the DSIM drives is given in Section 2, Section 3 is devoted to the development of a new discrete repetitive sliding model controller, Simulation results are presented in Section 4. Section 5 concludes.

II. Model of SPIM Drives

The drive system under study consists of a DSIM fed by a six-phase Voltage Source Inverter (VSI) and a DC link. A detailed scheme of the drive is provided in Fig. 1.

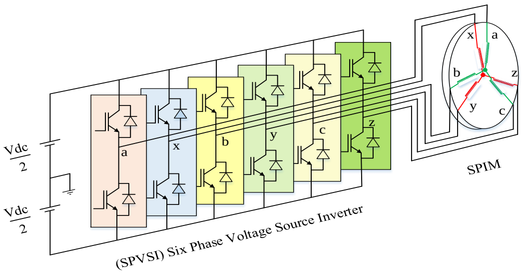

Fig. 1. A DSIM drives general diagram

By applying the Vector Space Decomposition (VSD) technique, the original six-dimensional space of the machine is transformed into three two-dimensional orthogonal subspaces in the stationary reference frame $(D-Q),(x - y)$ and $(z_l - z_2)$. This transformation is obtained by means of 6x6 transformation matrix eq. (1). To develop DSIM model for control purposes, some basic assumptions should be made. Hence, the windings are assumed to be sinusoidally distributed, the magnetic saturation, the mutual leakage inductances, and the core losses are neglected.

$$T_6 = \frac{1}{3}\begin{bmatrix} 1 & \frac{\sqrt{3}}{2} & -\frac{1}{2} & -\frac{\sqrt{3}}{2} & -\frac{1}{2} & 0 \\ 0 & \frac{1}{2} & \frac{\sqrt{3}}{2} & \frac{1}{2} & -\frac{\sqrt{3}}{2} & -1 \\ 1 & -\frac{\sqrt{3}}{2} & -\frac{1}{2} & \frac{\sqrt{3}}{2} & -\frac{1}{2} & 0 \\ 0 & \frac{1}{2} & -\frac{\sqrt{3}}{2} & \frac{1}{2} & \frac{\sqrt{3}}{2} & -1 \\ 1 & 0 & 1 & 0 & 1 & 0 \\ 0 & 1 & 0 & 1 & 0 & 1 \end{bmatrix} \quad (1)$$

The electrical matrix equations in the stationary reference frame for the stator and the rotor may be written as

$$\begin{aligned} [V_s] &= [R_s][I_s] + p([L_s][I_s] + [L_m][I_r]) \\ 0 &= [R_r][I_r] + p([L_r][I_r] + [L_m][I_s]) \end{aligned} \quad (2)$$

where: $[V],[I],[R],[L]$ and $[L_m]$ are voltage, current, resistant, self and mutual inductance vectors, respectively. p is differential operator. Subscript r and s related to rotor and stator resistance respectively. Since the rotor is squirrel cage, $[V]$ is equal to zero. The electromechanical energy conversion only takes place in the only takes place in the $D-Q$ subspace and the other subspaces just produce losses. Therefore, the control is based on determining the applied voltage in the DQ reference frame. With this transformation, the DSIM control technique is like the classical three phase IM FOC. The moment equation when expressed is as follows:

$$T_e = 3P(\psi_{rQ} i_{rD} - \psi_{rD} i_{rQ}) \quad (3)$$

where: $T_e, P, \Psi_{rD}, \Psi_{rQ}, i_{rD}, i_{rQ}$ are the electromagnetic torque, number of pole pairs, the rotor flux, and the rotor current, respectively. The control for the motor in the stationary reference frame is difficult, even for a three phase IM, so the transformation of DSIM model in a dq rotating reference frame to obtain currents with dc components is necessary, a transformation matrix must be used to represent the stationary reference fame (DQ) in the dynamic reference $(d - q)$. This matrix is given:

$$T_{dq} = \begin{bmatrix} cos(\delta) & -sin(\delta) \\ sin(\delta) & cos(\delta) \end{bmatrix} \quad (4)$$

where δ is the rotor angular position referred to the stator. In the FOC method, the rotor flux is controlled by isd stator current component and the torque by i_{sq} quadratic component. We have: $\psi_{rq} = 0; \psi_{rd} = \psi_{rd}$. The model motor dynamics is described by the following space vector differential equations:

$$\begin{cases} \frac{d\omega_r}{dt} = \frac{3}{2}P\frac{\delta\sigma L_s}{J}(\psi_{rd} i_{sq}) - \frac{T_L}{J} - B'_{\omega_r} \\ \frac{d\psi_{rd}}{dt} = \frac{L_m}{\tau_r} i_{sd} - \frac{1}{\tau_r}\psi_{rd} \\ L_s\frac{di_{sq}}{dt} = -ai_{sq} + L_s\omega_e i_{sd} + b\omega_e\psi_{rd} + cu_{sq} \\ L_s\frac{di_{sd}}{dt} = -ai_{sd} + L_s\omega_e i_{sq} + bR_r\psi_{rd} + cu_{sd} \end{cases} \quad (5)$$

where

$$\sigma = 1 - \frac{L_m^2}{L_s L_r}; \delta = \frac{L_m}{\sigma L_s L_r}; a = \frac{L_m^2 R_r + L_r^2 R_s}{\sigma L_r^2}; b = \frac{L_m^2 R_r}{\sigma L_r^2}; c = \frac{1}{\sigma}; \tau_r = \frac{L_r}{R_r}; B' = \frac{B}{J} \quad (6)$$

$u_{sd}, u_{sq}; i_{sd}, i_{sq}$: is the components of stator voltage and current, respectively; ψ_{rd}, ψ_{rq} is the rotor flux components; T_e, T_L is the electromagnetic and load torque; $d-q$ is synchronous and stationary axis reference frame quantities, respectively; ω_r is the angular velocity (mechanical speed), $\omega_r = \left(\frac{2}{P}\right)\omega_{re}$; $\omega_{re}, \omega_{sl}, \omega_e$ is the electrical speed respectively Rotor and slip angular and synchronous angular velocity; L_s, L_r is the stator and rotor inductances; L_m is the mutual inductance; R_s, R_r is the stator and rotor resistances; J is the inertia of motor and load; σ is the total linkage coefficient; B is the friction coefficient; τ_r is the rotor and stator time constant.

The electromagnetic torque and the slip frequency can be expressed in dq reference frame:

$$T_e = \frac{3P}{2}\frac{L_m}{L_r}\psi_{rd} i_{sq}; \ \omega_{sl} = \frac{M}{L_r}\psi_{rd} i_{sq} \quad (7)$$

III. DRVGSTASOSM Structure for FOC DSIM Drives

A. Design the Outer Speed And Flux Loop

As we have seen, classic SM provides robust and high-accuracy solutions for a wide range of control problems under uncertainty conditions. However, the main restriction remains that high-frequency control switching may easily cause unacceptable practical complications (chattering effect), if the control has any physical sense [59]-[60]. To overcome this problem, in the proposed controller, we propose using improved order second sliding technique, that is developed based on [60]. The second order slip surface according to the rotor flux, speed components are defined as follows:

$$S_m(k)=\begin{bmatrix}s_1(k)\\ s_2(k)\end{bmatrix}=\begin{bmatrix}\varepsilon_{\psi rd}+\lambda_4.\left|\varepsilon_{\psi rd}\right|^{1/2}sat(\varepsilon_{\psi rd})\\ \varepsilon_{\omega r}+\lambda_3.\left|\varepsilon_{\omega r}\right|^{1/2}sat(\varepsilon_{\omega r})\end{bmatrix} \tag{8}$$

where: $\lambda_{1,2}$ are positive coefficients. The rotor flux, speed are defined

$$\begin{cases}\varepsilon_{\psi rd}=\psi_{rd}^*-\psi_{rd}\\ \varepsilon_{\omega r}=\omega_r^*-\omega_r\end{cases} \tag{9}$$

In the presence of periodic disturbances, the second order sliding mode control performances are decreased considerably. To deal with this problem, the combination the repetitive control with improved SOSM control is developed based on [59]. We suppose that the disturbances vector $d_m(k)$ is periodic with the period N:

$$d_m(k)=\begin{bmatrix}d_1(k)\\ d_2(k)\end{bmatrix}=\begin{bmatrix}d_1(k-N)\\ d_2(k-N)\end{bmatrix}=d_m(k-N) \tag{10}$$

Based on condition of disturbance rejection [59], the sliding functions vector is then given as follows:

$$S_m(k+1)=\phi S_m(k)+\begin{bmatrix}\mu_1 sat(s_1(k))\\ \mu_2 sat(s_2(k))\end{bmatrix}+\gamma[d_m(k)-d_m(k-N)] \tag{11}$$

where: $\mu_{1,2}$ are positive coefficients.

The control expression of the new system is

$$[u(k)]=[u_m(k)+u_m^{dis}(k)] \tag{12}$$

where: vector $[u_m(k)]$ are designed based on VGSTA [60], and they are defined as (13):

$$[u_m(k)]=\begin{bmatrix}u_1(k)\\ u_2(k)\end{bmatrix}=\begin{bmatrix}k_1(t,\varepsilon_{\mathrm{isd}})\left(\delta_1(s_1(k))+\int_0^t\delta_2(s_1(k))\,dt\right)\\ k_2(t,\varepsilon_{\mathrm{isd}})\left(\delta_3(s_2(k))+\int_0^t\delta_4(s_2(k))\,dt\right)\end{bmatrix} \tag{13}$$

where:

$k_1(t,\varepsilon_{\mathrm{isd}})=S_1 sat(S_1);\delta_1(s(k))=|s_1(k)|^{1/2}.sat(s_1(k))+k_\lambda.s_1(k);$

$\delta_2(s(k))=\frac{1}{2}.sat(s_1(k))+\frac{3}{2}k_\lambda|s_1(k)|^{1/2}.sat(s_1(k))+k_\lambda^2.s_1(k)$

$k_2(t,\varepsilon_{\mathrm{isq}})=S_2 sat(S_2);\delta_3(s(k))=|s_2(k)|^{1/2}.sat(s_2(k))+k_\lambda.s_2(k)$

$\delta_4(s(k))=\frac{1}{2}.sat(s_2(k))+\frac{3}{2}k_\lambda|s_2(k)|^{1/2}.sat(s_2(k))+k_\lambda^2.s_2(k)$

$[u_m^{dis}(k)]$ are the disturbance vectors be given the system to cancel periodic disturbances and they are defined:

$$[u_m^{dis}(k)]=\begin{bmatrix}u_1^{dis}(k)\\ u_2^{dis}(k)\end{bmatrix}=\begin{bmatrix}\varepsilon_{\psi rd}(k)+\gamma_1 sat(s_1(k+1))\\ \varepsilon_{\omega r}(k)+\gamma_2 sat(s_2(k+1))\end{bmatrix} \tag{14}$$

where: $\gamma_{1,2,3,4}$ are positive coefficients. Lyapunov functions are chosen:

$$V=\frac{1}{2}[V_1^2+V_2^2]=\frac{1}{2}[s_1(k)^2+s_2(k)^2] \tag{15}$$

Differentiate both sides equation (15) we get:

$$\frac{dV}{dt}=\left[s_1(k)\frac{ds_1(k)}{dt}+s_2(k)\frac{ds_2(k)}{dt}\right] \tag{16}$$

$$\begin{cases}\frac{ds_1(k)}{dt}=\frac{d\left[\varepsilon_{\psi rd}+\lambda_1.\left|\varepsilon_{\psi rd}\right|^{1/2}sat(\varepsilon_{\psi rd})\right]}{dt}\\ \frac{ds_2(k)}{dt}=\frac{d[\varepsilon_{\omega r}+\lambda_2.|\varepsilon_{\omega r}|^{1/2}sat(\varepsilon_{\omega r})]}{dt}\end{cases}$$
$$\Rightarrow\begin{cases}\frac{ds_1(k)}{dt}=\frac{d[\psi_{rd}^*-\psi_{rd}]}{dt}+\frac{d\left[\lambda_1.\left|\varepsilon_{\psi rd}\right|^{1/2}sat(\varepsilon_{\psi rd})\right]}{dt}\\ \frac{ds_2(k)}{dt}=\frac{d[\omega_r^*-\omega_r]}{dt}+\frac{d[\lambda_2.|\varepsilon_{\omega r}|^{1/2}sat(\varepsilon_{\omega r})]}{dt}\end{cases} \tag{17}$$

On the other hand, to satisfy the stability condition according to Lyapunov theory, the sliding surface differential function is chosen as follows:

$$\frac{ds_m(k)}{dt}=-[u_m(k)+u_m^{dis}(k)] \tag{18}$$

Combining expressions Eq. (16) to (18), i_{sd}^*,i_{sq}^* virtual vectors are chosen for the outer speed and flux loop (19).

$$\begin{cases}i_{sd}^*(k)=\frac{\tau_r}{L_m}\left\{\frac{d\psi_{rd}^*}{dt}+\frac{1}{\tau_r}\psi_{rd}+\frac{d\left[\lambda_1.\left|\varepsilon_{\psi rd}\right|^{1/2}sat(\varepsilon_{\psi rd})\right]}{dt}+\left[u_1(k)+u_1^{dis}(k)\right]\right\}\\ i_{sq}^*(k)=\frac{1}{k_{sq}\psi_{rd}}\left\{\frac{d\omega_r^*}{dt}+\frac{T_L}{J}+B^{'}\omega_r+\frac{d\left[\lambda_2.|\varepsilon_{\omega r}|^{1/2}sat(\varepsilon_{\omega r})\right]}{dt}+\left[u_2(k)+u_2^{dis}(k)\right]\right\}\end{cases} \tag{19}$$

i_{sd}^* and i_{sq}^* virtual control vectors in Eq. (19) are chosen to satisfy the control objectives and these virtual components also provide as the reference inputs for calculating u_{sd}^*,u_{sq}^* virtual control vectors. Ψ_{rd} rotor flux is identified by curent model. The load torque T_L is estimated:

$$\hat{T}_L=\frac{1}{1+\tau_0 p}\left[\left(\frac{3}{2}\right)P\frac{L_m}{L_r}\hat{\psi}_{rd}i_{sq}-\frac{J}{P}\frac{d\omega}{dt}\right] \tag{20}$$

where: τ_0 is time gain; p is the differential.

B. Design the Inner Current Loop Controls:

The improved nonlinear slip surface according to the current components are defined as follows:

$$S_m(k) = \begin{bmatrix} s_3(k) \\ s_4(k) \end{bmatrix} = \begin{bmatrix} \varepsilon_{isd} + \lambda_1.\left|\varepsilon_{isd}\right|^{1/2} sat(\varepsilon_{isd}) \\ \varepsilon_{isq} + \lambda_2.\left|\varepsilon_{isq}\right|^{1/2} sat(\varepsilon_{isq}) \end{bmatrix} \quad (21)$$

where: $\lambda_{3,4}$ are positive coefficients. The stator current errors are defined

$$\begin{cases} \varepsilon_{isd} = i_{sd}^* - i_{sd} \\ \varepsilon_{isq} = i_{sq}^* - i_{sq} \end{cases} \quad (22)$$

We suppose that the disturbances vector $d_m(k)$ is periodic with the period N:

$$d_m(k) = \begin{bmatrix} d_3(k) \\ d_4(k) \end{bmatrix} = \begin{bmatrix} d_3(k-N) \\ d_4(k-N) \end{bmatrix} = d_m(k-N) \quad (23)$$

Based on condition of disturbance rejection [49], the sliding functions vector is then given as follows:

$$\begin{aligned} S_m(k+1) = \phi S_m(k) + \begin{bmatrix} \mu_3 sat(s_3(k)) \\ \mu_4 sat(s_4(k)) \end{bmatrix} \\ + \quad \gamma[d_m(k) - d_m(k-N)] \end{aligned} \quad (24)$$

where: $\mu_{3,4}$ are positive coefficients. The control expression of the new system is

$$[u(k)] = [u_m(k) + u_m^{dis}(k)] \quad (25)$$

where: vector $[u_m(k)]$ are designed based on the VGSTA [60], and they are defined as follow:

$$\begin{aligned} [u_m(k)] &= \begin{bmatrix} u_3(k) \\ u_4(k) \end{bmatrix} \\ &= \begin{bmatrix} k_3(t, \varepsilon_{isd}) = S_1 sat(S_1)\left(\delta_5(s_3(k)) + \int_0^t \delta_6(s_3(k))\, dt\right) \\ k_4(t, \varepsilon_{isd}) = S_1 sat(S_1)\left(\delta_7(s_4(k)) + \int_0^t \delta_8(s_4(k))\, dt\right) \end{bmatrix} \end{aligned} \quad (26)$$

where:

$k_3(t, \varepsilon_{isd}) = S_3 sat(S_3); \delta_5(s(k)) = |s_3(k)|^{1/2}.sat(s_3(k)) + k_\lambda.s_3(k);$

$\delta_6(s(k)) = \frac{1}{2}.sat(s_3(k)) + \frac{3}{2}k_\lambda|s_3(k)|^{1/2}.sat(s_3(k)) + k_\lambda^2.s_3(k);$

$k_4(t, \varepsilon_{isd}) = S_4 sat(S_4); \delta_7(s(k)) = |s_4(k)|^{1/2}.sat(s_4(k)) + k_\lambda.s_4(k);$

$\delta_8(s(k)) = \frac{1}{2}.sat(s_4(k)) + \frac{3}{2}k_\lambda|s_4(k)|^{1/2}.sat(s_4(k)) + k_\lambda^2.s_4(k)$

$[u_m^{dis}(k)]$ are the disturbance vectors be given the system to cancel periodic disturbances and they are defined:

$$\begin{aligned} [u_m^{dis}(k)] &= \begin{bmatrix} u_3^{dis}(k) \\ u_4^{dis}(k) \end{bmatrix} \\ &= \begin{bmatrix} \varepsilon_{isd}(k) + \gamma_3 sat(s_3(k+1)) \\ \varepsilon_{isq}(k) + \gamma_4 sat(s_4(k+1)) \end{bmatrix} \end{aligned} \quad (27)$$

where: $\gamma_{1,2,3,4}$ are positive coefficients. Lyapunov functions are chosen:

$$V = \frac{1}{2}[V_3^2 + V_4^2] = \frac{1}{2}[s_3(k)^2 + s_4(k)^2] \quad (28)$$

Differentiate both sides equation (15) we get:

$$\frac{dV}{dt} = \left[s_3(k)\frac{ds_3(k)}{dt} + s_4(k)\frac{ds_4(k)}{dt}\right] \quad (29)$$

$$\begin{aligned} &\begin{cases} \dfrac{ds_3(k)}{dt} = \dfrac{d\left[\varepsilon_{isd} + \lambda_3.|\varepsilon_{isd}|^{1/2} sat(\varepsilon_{isd})\right]}{dt} \\ \dfrac{ds_4(k)}{dt} = \dfrac{d\left[\varepsilon_{isq} + \lambda_4.\left|\varepsilon_{isq}\right|^{1/2} sat(\varepsilon_{isq})\right]}{dt} \end{cases} \\ \Rightarrow &\begin{cases} \dfrac{ds_3(k)}{dt} = \dfrac{d[i_{sd}^* - i_{sd}]}{dt} + \dfrac{d\left[\lambda_3.|\varepsilon_{isd}|^{1/2} sat(\varepsilon_{isd})\right]}{dt} \\ \dfrac{ds_4(k)}{dt} = \dfrac{d[i_{sq}^* - i_{sq}]}{dt} + \dfrac{d\left[\lambda_4.\left|\varepsilon_{isq}\right|^{1/2} sat(\varepsilon_{isq})\right]}{dt} \end{cases} \end{aligned} \quad (30)$$

On the other hand, to satisfy the stability condition according to Lyapunov theory, the sliding surface differential function is chosen as follows:

$$\frac{ds_m(k)}{dt} = -[u_m(k) + u_m^{dis}(k)] \quad (31)$$

Combining expressions Eq. (29) to (31), u_{sd}^*, u_{sq}^* virtual control vectors are chosen as (32).

C. Stability Analysis

The Lyapunov function of the system is defined in expression (15), taking the differentiation of both sides of the Lyapunov function we get expression (16). Combining expression (16), (17), (18) we get (33).

$$\begin{cases} u_{sd}^*(k) = \dfrac{L_s}{c}\left\{\dfrac{di_{sd}^*}{dt} + a i_{sd} - L_s\omega_e i_{sq} - b\psi_{rd} + \dfrac{d\left[\lambda_3.|\varepsilon_{isd}|^{1/2} sat(\varepsilon_{isd})\right]}{dt} + \left[u_3(k) + u_3^{dis}(k)\right]\right\} \\ u_{sq}^*(k) = \dfrac{L_s}{c}\left\{\dfrac{di_{sq}^*}{dt} + a i_{sq} - L_s\omega_e i_{sd} - b_r\omega_e\psi_{rd} + \dfrac{d\left[\lambda_4.\left|\varepsilon_{isq}\right|^{1/2} sat(\varepsilon_{isq})\right]}{dt} + \left[u_4(k) + u_4^{dis}(k)\right]\right\} \end{cases} \quad (32)$$

where: $\lambda_{3,4}$; $\mu_{3,4}$; $\gamma_{3,4}$ are positive coefficients

$$\frac{dV}{dt} = -\begin{bmatrix} s_1(k)\left[u_1(k) + u_1^{dis}(k)\right] + s_2(k)\left[u_2(k) + u_2^{dis}(k)\right] \\ +s_3(k)\left[u_3(k) + u_3^{dis}(k)\right] + s_4(k)\left[u_4(k) + u_4^{dis}(k)\right] \end{bmatrix} \quad (33)$$

With,

$$\begin{cases} [s_1(k)] = \left[\varepsilon_{\psi rd} + \lambda_1.\left|\varepsilon_{\psi rd}\right|^{1/2} sat(\varepsilon_{\psi rd})\right] \\ [u_1(k)] = \begin{bmatrix} k_1(t,x).\,\delta_1(s_1(k)) \\ \quad + \int_0^t k_2(t,x).\,\delta_2(s_1(k))\,dt \end{bmatrix} \\ \left[u_1^{dis}(k)\right] = \varepsilon_{\psi rd}(k) + \gamma_1 sat(s_1(k+1)) \end{cases}$$
$$\Rightarrow s_1(k)\left[u_1(k) + u_1^{dis}(k)\right] > 0 \forall \varepsilon_{\psi rd};$$

$$\begin{cases} [s_2(k)] = \left[\varepsilon_{\omega r} + \lambda_3.\left|\varepsilon_{\omega r}\right|^{1/2} sat(\varepsilon_{\omega r})\right] \\ \begin{bmatrix} k_3(t,x).\,\delta_3(s_2(k)) \\ \quad + \int_0^t k_4(t,x).\,\delta_4(s_2(k))\,dt \end{bmatrix} \\ \left[u_2^{dis}(k)\right] = \varepsilon_{\omega r}(k) + \gamma_3 sat(s_3(k+1)) \end{cases}$$
$$\Rightarrow s_2(k)\left[u_2(k) + u_2^{dis}(k)\right] > 0 \forall \varepsilon_{\omega r}$$

$$\begin{cases} [s_3(k)] = \left[\varepsilon_{isd} + \lambda_3.\left|\varepsilon_{isd}\right|^{1/2} sat(\varepsilon_{isd})\right] \\ [u_3(k)] = \begin{bmatrix} k_5(t,x).\,\delta_5(s_3(k)) \\ \quad + \int_0^t k_6(t,x).\,\delta_6(s_3(k))\,dt \end{bmatrix} \\ \left[u_1^{dis}(k)\right] = \varepsilon_{\psi rd}(k) + \gamma_1 sat(s_1(k+1)) \end{cases}$$
$$\Rightarrow s_4(k)\left[u_4(k) + u_4^{dis}(k)\right] > 0 \forall \varepsilon_{isq};$$

$$\begin{cases} [s_4(k)] = \left[\varepsilon_{isq} + \lambda_4.\left|\varepsilon_{isq}\right|^{1/2} sat(\varepsilon_{isq})\right] \\ \begin{bmatrix} k_7(t,x).\,\delta_7(s_4(k)) \\ \quad + \int_0^t k_8(t,x).\,\delta_8(s_4(k))\,dt \end{bmatrix} \\ \left[u_4^{dis}(k)\right] = \varepsilon_{isq}(k) + \gamma_2 sat(s_4(k+1)) \end{cases}$$
$$\Rightarrow s_4(k)\left[u_4(k) + u_4^{dis}(k)\right] > 0 \forall \varepsilon_{isq}$$

From equation (33) we get:

$$\frac{dV}{dt} < 0 with \forall \{\lambda; \gamma; \mu > 0\} \tag{34}$$

Thus, the system is always stable according to Lyapunov stability theory.

IV. SIMULINK AND DISCUSSION

The performance of the DRRISOSM controller for FOC vector control of SPIM drives is validated through simulation using MATLAB software. To increase the reliability, comparison frameworks are established, similar surveys are also implemented for SOSM control in [30], this comparison to make clearly the second order sliding mode control shows that then combination RC control and improved SOSM control give a deal has superior performance in terms of harmonic immunity and accurate tracking of the reference speed, the PI controller is also chosen to make the create comparison data because it is now still the standard solution and the most widely used solution in industry and in engineering practice. Additionally, DRRISOSM control also is compared with other latest methods in [37], [49], to confirm quantify the effectiveness of the proposed control structure. The block diagram of the SPIM drive system is shown in Fig. 2. In these simulations, a six-phase squirrel-cage type IM with the rated parameters are given as follow: 1HP, 6-phase, 220 *V*, 50 *Hz*, 4 poles, 1450 *rpm*. R_s =10.1Ω, R_r =9.8546Ω, L_s =0.833457H, L_r =0.830811H, L_m =0.783106H, J = 0.0088 *kg.m*^{2}. Setting the Sampling Time T_s =1e-5 sec; and set T_s (1e-5 sec) for the step size parameter.

A. The Dynamic Performance of Proposed Controller Under Variable Speeed and Torque Disturbance

The starting and reversing mode investigation was carried out to confirm the dynamic performance of DR VGSTASOSM controller. The speed, torque, current and rotor flux responses are shown in Fig. 3. The reference speed increases from 0 to1440 *rpm* at t=0.5s; reversed to -1440*rpm* then decreased to 0 at t= 3, 4*s*, respectively, and increased to 100 *rpm* at t= 5.5*s*, rated load applied at t = 1.5s. This survey was carried out based on the experiments in [37], in that a hybrid nonlinear control which is composed of the super twisting algorithm (STA) based second order sliding mode control applying fuzzy logic method (FSOSMC) has been proposed. This Test is also carried out with the PI and SOSM controllers [30] to get comparison data.

In this proposal, to deal with the torque ripple and load disturbance, a DRVGSTASOSM control strategy with improved SOSM comminating with RC is proposed as in part 3. Observation of the obtained results shows that the DR VGSTASOSM controller can provide faster dynamic responses and stabilization time. The start-up time of DSIM from 0 to 1440 *rpm* in the case of the drive system using PI, SOSM and DR VGSTASOSM controllers are 0.15*s* and 0.12*s* and 0.097s, respectively. At t =1.5 s, the rated torque is applied, the load disturbance negatively affects the performance on the PI controller causing a sudden speed drop of 25.43 rpm (1.77%) and 0.125*s* to stabilize, steady state error 3.89 *rpm* (0.27 %). The load disturbance also impacted to the performance of both SOSM and the proposed controler, but these both control strategies control quite well, the speed distortions were not too serious due to the load disturbance is identified and put into both SOSM and DRVGSTASOSM, it indirectly helps effectively reconstructed the load disturbance and allowes both control faster compensation than PI control. The transient parameters of SOSM and DRVGSTASOSM are the same when applying load disturbance and are the sudden 11.71 rpm (0.81% drop) speed drop, 0.009s to stabilize. At time t=1.5s, the speed is reversed directly from 1440 rpm to -1440 rpm. As soon as the speed reversal is applied, the torque is immediately reversed, the motor starts to decelerate to reach 0 speed and then accelerates in the opposite direction and stabilizes at -1440 rpm. The total reversal time of the DSIM drive system using PI, SOSM and DR VGSTASOSM controllers are 0.198s, 0.147s and 0.139s respectively. When observing FSOSMC controller in Fig. 5 to Fig. 6, [37] shows this strategy also performs the good reversal, however, torque and rotor flux oscillation appear during the survey, the chattering phenomenon has not been eliminated.

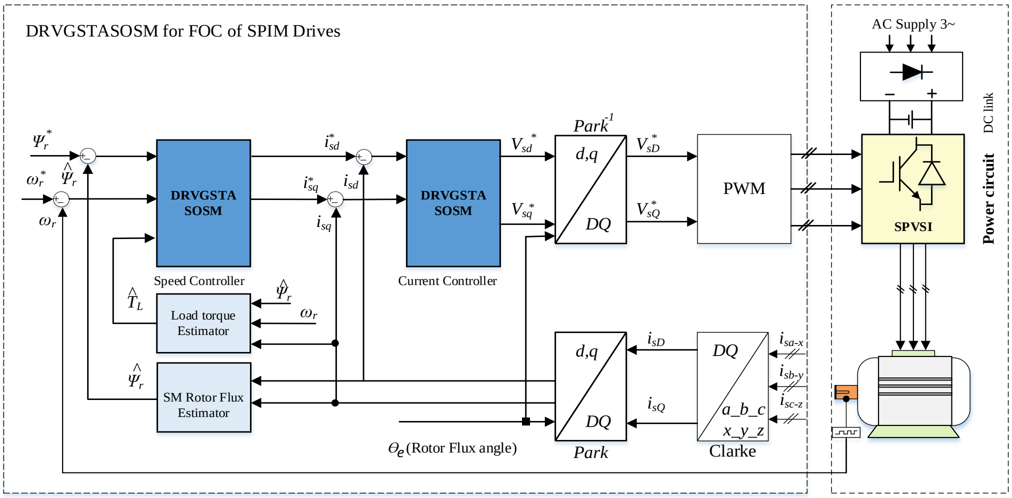

Fig. 2. FOC Vector control of SPIM drive using DRRISOSM control structure

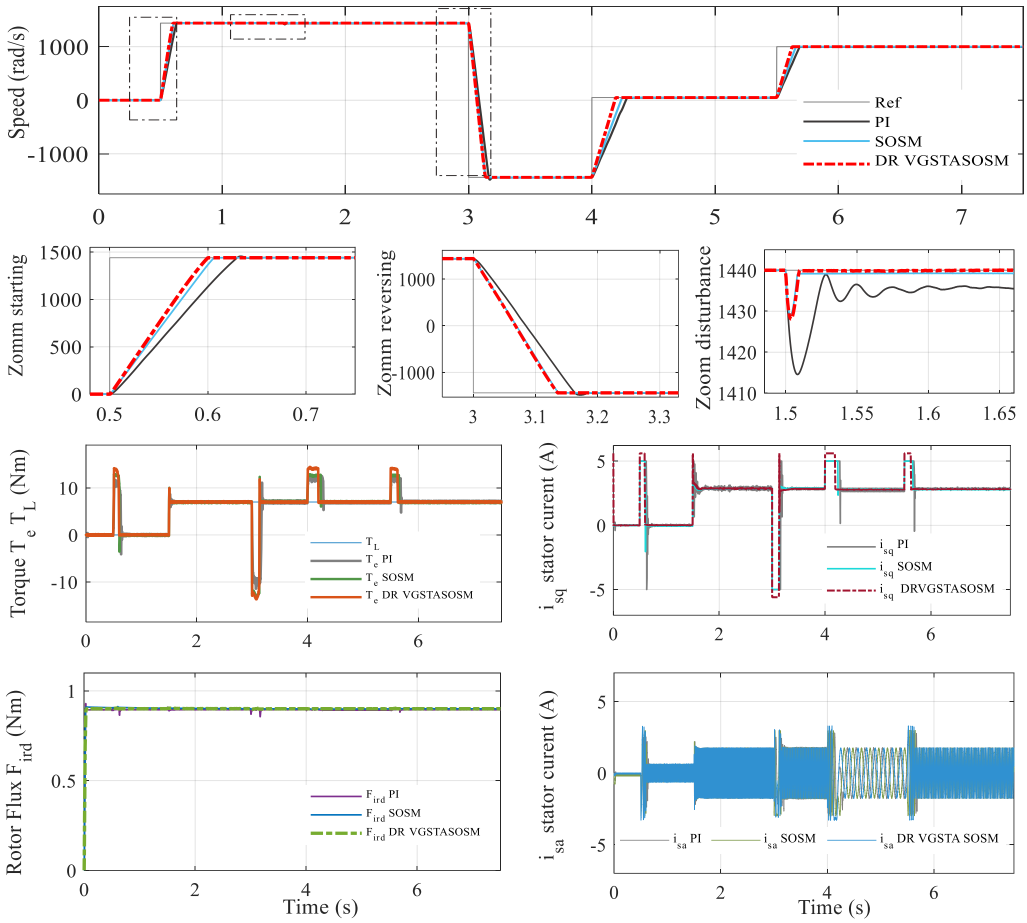

Fig. 3. Performance of PI, SOSM and DRVGSTASOSM controllers under the variable speed

B. Test for Robustness Against Harmonic Disturbance

To validate the robustness of the proposed controller, a test is implemented with the motor load that has a significant cogging torque due to motor and load were coupled by a below coupler, where appearing considerable misalignment [49]. The drive system has strong torque harmonic components; the most significant orders are the first, fourth and 12th. The first and fourth harmonics are present due to the misalignment of the system and the12th harmonic is generated by the mutual torque and cogging components of the load both at the same frequency [49]. In this part, the speed was surveyed at 100 *rpm* and 600 rpm with extended harmonics load is activated at t=1s. The harmonic torque disturbance can be described in terms of the rotor position, θ, as

$$T_d(k) = T_c\, cos(m\theta) + T_s\, sin(m\theta) \tag{35}$$

where T_s, T_c are the mth harmonic sine and cosine components.

In this case, at 100 and 600 rpm speed, the harmonic frequencies appear 1.66, 6.66, 20 *Hz* and at 10, 40 and 120 *Hz*, respectively, (the first, fourth, and 12*th* harmonic orders). The speed, torque responses of PI, SOSM, DR VGSTASOSM controllers for 100 and 600 rpm is shown in Fig. 4. From the surveyed results show that the PI strategy attempted to control the speed, however, with fixed Kp, Ki coefficients and the absence of torque estimation component in the control process so the performance of the control was significantly reduced when appearing harmonic disturbances, it has the largest speed, torque current oscillation. SOSM controls quite well in normal torque disturbance cases, but harmonic disturbance appears, SOSM cannot operate stably, the speed, torque current oscillations increases but with smaller oscillation than PI controller. Comparing the results achieved in Fig. 4, Fig. 5, [49] using adaptive feedforward controller (AFC) shows that AFC cannot reject all external disturbance. On the contrary, DR VGSTASOSM control eliminates the harmonic disturbance very well, the drive using this proposed control operates robustly and is almost unaffected when harmonic disturbance appears for two cases 100 and 600 rpm.

The performance of the proposed controller in the speed variation condition is demonstrated in Fig. 5. First, the DSIM operates at 100 rpm, then increases to 300, 600 at $t = 5$, 10s and decreases successively to 300, 100 *rpm* at $t = 15$, 20s, respectively. Comparing the speed responses in Fig. 5, we see that PI controllers give large speed oscillation, the drive system operates unstably, AFC controller in Fig. 14, [49] significantly decreases the harmonic disturbances without instability. On the contrary, DRVGSTASOSM provides very good response, the drive system operates robustly and is not affected by harmonic disturbance, the stability of the system is guaranteed due to the design process based on Lyapunov stability theory.

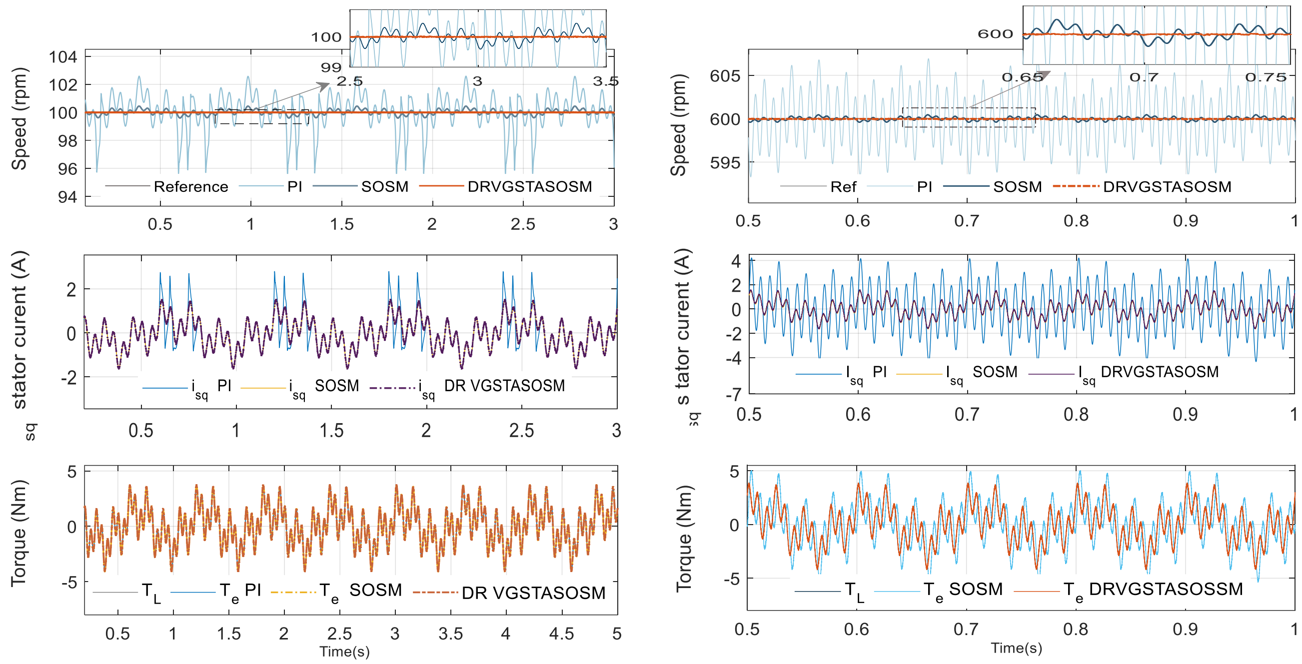

Fig. 4. The speed, torque, isq torque current responses of PI, SOSM, DR VGSTASOSM under harmonic torque disturbance at 100 rpm b. at 600 rpm

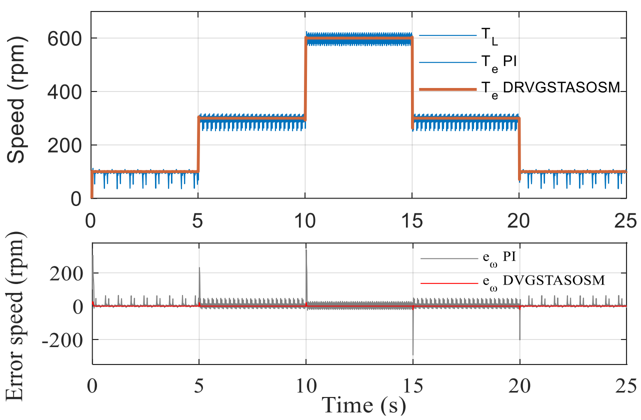

Fig. 5. Performance of DR VGSTASOSM controller under variable speed and harmonic load disturbance

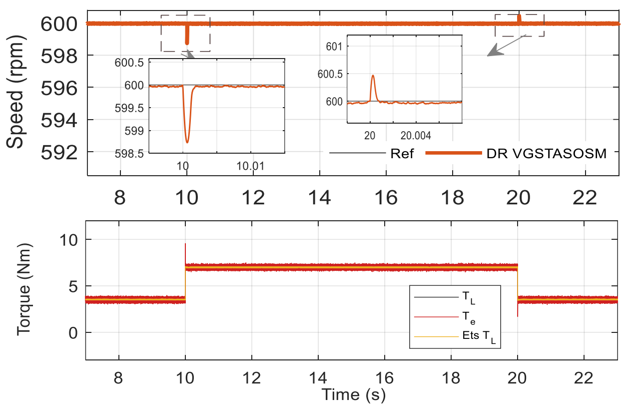

Fig. 6. Performance of DRVGSTASOSM controller under constant speed and step load disturbance

Another test also was performed with the speed kept constant at 600 *rpm*. At the moment of sudden applied load, the speed of motor is decreasing rapidly 1.25 *rpm* (0.002%) and then it recovers in about 0.0018 s, at $t = 20$s, the load is rejected, the speed increases 0.41*rpm* (0.0007%) and then it recovers in about 0.0058s. The SS error is almost zero. From the simulink results confirmed the tracking and harmonic disturbance rejection performance also robustness of the proposed DR VGSTASOSM controller.

C. *Test for Robustness Against SPIM Parametric Uncertainties*

In order to verify and confirm more clearly the robustness of the DR VGSTASOSM controller to load disturbances and the impact of DSIM parameter changes, another survey was conducted under load disturbance conditions, the machine parameters R_s, R_r will be changed in the high-speed range, R_s increases at t= 1.5*s* to 1.5 times normal stator resistance and R_r increases to 1.5 times to 2 times the normal rotor resistance at t= 1.5*s* and t= 2.5*s*, respectively. The speed is kept constant at 1000 *rpm* with a rated load.

Comparing the results obtained in Fig. 7 shows that at t=1.5*s* when R_s, R_r increase 150% normal stator and rotor resistance, the controllers are all adaptive when operating uncertain parameters. However, the performance of the DR VGSTASOSM controller are the better, this controller give the speed stably and exactly reference tracking in during the investigation period, and disturbances and fluctuations in speed, torque and flux are almost non-existent, the speed, torque and flux respones of PI controller affected by R_r, R_s resistance changes. At the moment t=2.5, R_r increase to 200% normal rotor resistance, R_s kept 150% normal stator resistance, we see that the DR VGSTASOSM stratergy controls the speed very well even though very severe working conditions, on the contrary, with PI controller appears the speed, torque and flux oscillations.

D. *Test for Robustness Against Open Circuit Fault*

To confirm the performance and the robustness under open circuit fault at low speed. The survey is conducted with DSIM works at constant speed (100*rpm*) with rated load torque under open phase fault at t=0.5 s (phase an opened). Fig. 8 shows the speed, torque and current corresponding for PI and the proposed DR VGSTASOSM controller. At time t=0.5s phase a of the DSIM is opened, PI controller is severely affected causing loss of convergence and stability when the fault appears. In contrast, because RC and improves SOSM made to both loop control, the proposed DR VGSTASOSM shows superior robustness, stability and high-speed convergence.

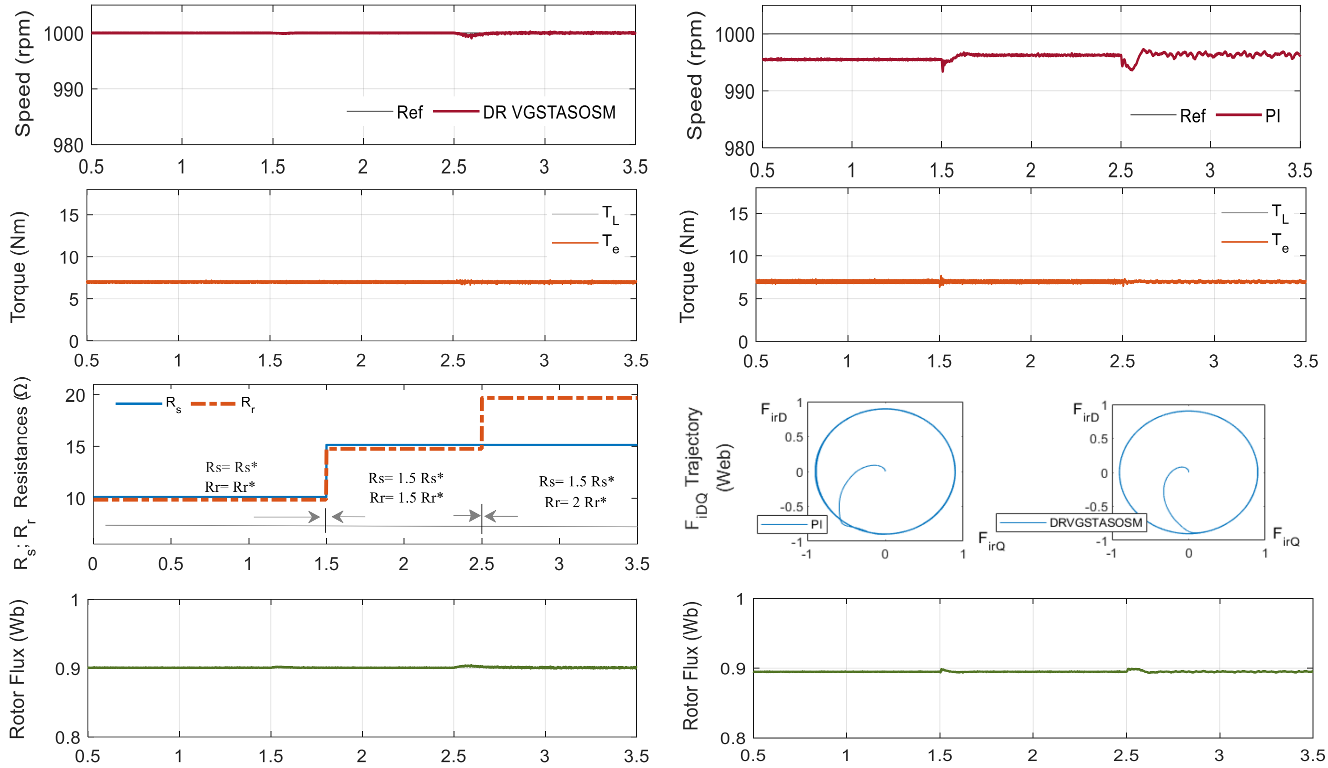

Fig. 7. The speed, torque, flux response when parameters *Rs, Rr* change

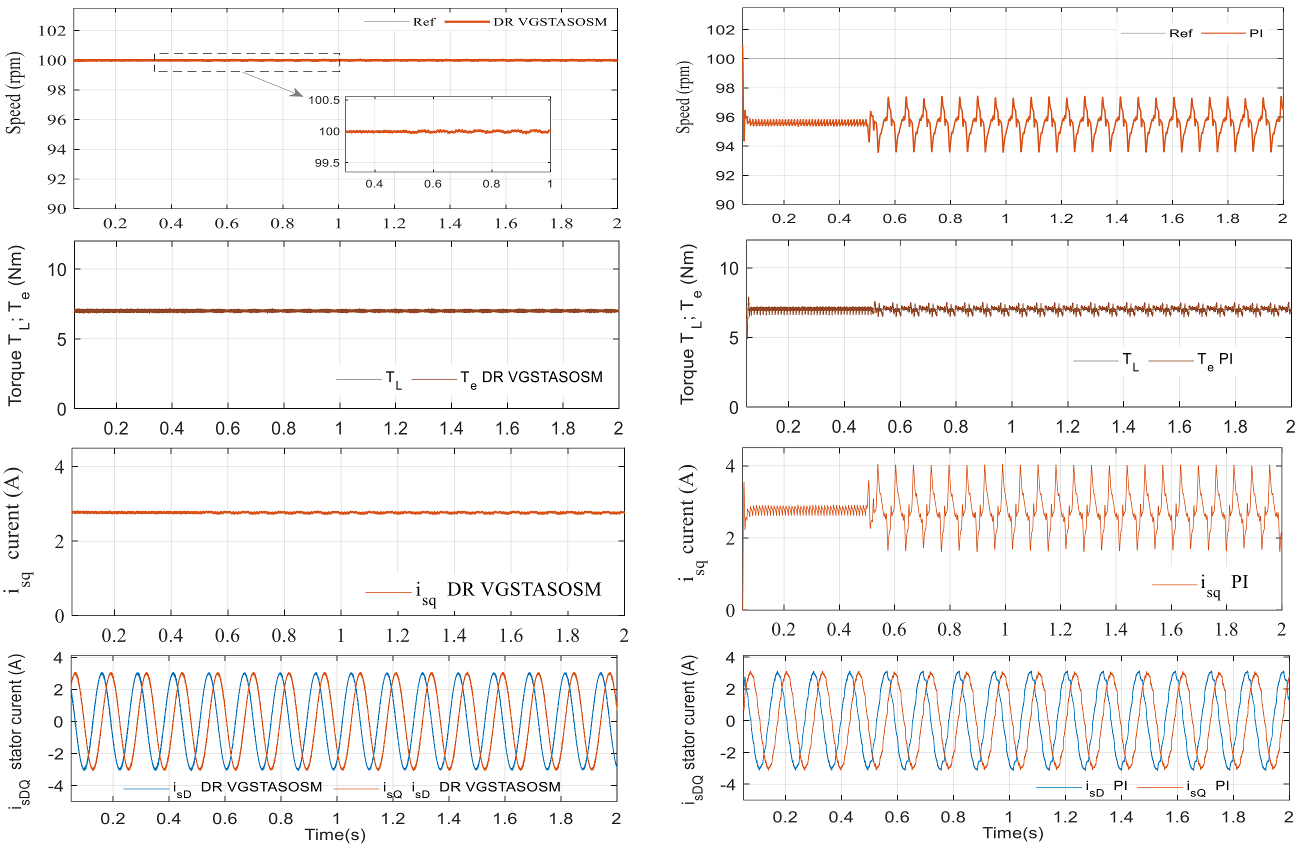

Fig. 8. The speed, torque, current responses under open phase fault (phase an opened)

V. CONCLUSION

This paper proposes an improved hybrid control structure by embedding the variable-gain super twisting algorithm into the improved second order sliding mode control and integrating plug-in repetitive control into this VSTASOSM structure made the control process becomes more adaptive and robust, allowing precise tracking and reducing the chattering phenomena, it also helps to effectively eliminates most overshoot, increases torque and speed response ability, reduces the influence of load disturbance and uncertain parameter, and proactively eliminates harmonic disturbances effectively . By minimizing mechanical stress during speed transitions, the proposed strategy not only improves tracking and stability but also contributes to extending the lifespan of the motor. The simulation results obtained by using MATLAB and the analysis, comparison data in sect. 4 have confirmed the effectiveness of the proposed control strategy for vector control of DSIM drives, It proves the improved tracking performance, harmonic disturbance rejection, and robust operation of the DSIM under varying conditions. In the future, I will continue to research and develop the hardware to address the experimental validation of this proposed DR VSTASOSM control strategy.

REFERENCES

[1] E. Levi, "Multiphase Electric Machines for Variable-Speed Applications," in *IEEE Transactions on Industrial Electronics*, vol. 55, no. 5, pp. 1893-1909, May 2008.

[2] A. Oumar, R. Chakib, M. Labbadi, and M. Cherkaoui, “Robust Nonlinear Controller of the Speed for Double Star Induction Machine in the Presence of a Sensor Fault,” *I. J. of Intell. Eng. and Syst*. vol. 13, no. 3, pp. 124-133, 2022.

[3] H. Chaabane, K. D. Eddine, and C. Salim, “Sensorless backstepping control using a Luenberger observer for double-star induction motor,” *Archives of Electrical Eng*., vol. 69, no. 1, pp. 101-116, 2020.

[4] A. M. Mahmoud, K. Houari, and A. Ma’arif, “Robust Flux and Speed State Observer Design for Sensorless Control of a Double Star Induction Motor,” *Journal of Robotics and Control*, vol. 3, no. 4, pp. 464-475, 2022.

[5] C. S. Lim, S. S. Lee, and E. Levi, "Continuous-Control-Set Model Predictive Current Control of Asymmetrical Six- Phase Drives Considering System Nonidealities," *IEEE Trans on Ind. Electron*., vol. 70, no. 8, pp. 7615-7626, 2023.

[6] S. Adigintla, M. V. Aware, and N. Arun, "Fractional Order Transfer Function Identification of Six-Phase Induction Motor Using Dual-Chirp Signal," *IEEE J. of Emerging and Selected Topics in Power Electron*., vol. 11, no. 5, pp. 5183-5194, 2023.

[7] N. T. Pham, “Design of Novel STASOSM Controller for FOC Control of Dual Star Induction Motor Drives,” *International Journal of Robotics and Control Systems*, vol. 4, no. 3, pp. 1059-1074, 2024.

[8] T. N. -C. Tran, H. X. Nguyen, J. W. Park, and J. W. Jeon, "A Stable Adaptive Gradient Descent Harmonic-Disturbance Rejection for Improving Phase-Tracking Accuracy," *IEEE Access*, vol. 8, pp. 31409-31419, 2020.

[9] N. T. Pham and T. D. Le, “Disturbance Rejective Repetitive Improved Second Order Sliding Mode Control for High Performance SPIM Drives,” *I. J. of Intell. Eng. and Syst.*, vol. 17, no. 6, 2024.

[10] W. Deng, X. Zhang, and B. Yan, "An Enhanced Discrete Virtual Vector-Based Direct Torque Control of PMSM Drives," *IEEE Trans on Energy Conversion*, vol. 39, no. 1, pp. 277-286, 2024.

[11] W. Wang, C. Liu, H. Zhao, and Z. Song, "Improved Deadbeat-Direct Torque and Flux Control for PMSM With Less Computation and

Enhanced Robustness," *IEEE Trans on Ind. Electron.*, vol. 70, no. 3, pp. 2254-2263, 2023.

[12] A. Nasr, C. Gu, X. Wang, G. Buticchi, S. Bozhko, and C. Gerada, "Torque-Performance Improvement for Direct Torque-Controlled PMSM Drives Based on Duty-Ratio Regulation," *IEEE Trans on Power Electron.*, vol. 37, no. 1, pp. 749-760, 2022.

[13] X. Sun *et al*., "Optimal Design of Terminal Sliding Mode Controller for Direct Torque Control of SRMs," *IEEE Transactions on Transportation Electrification*, vol. 8, no. 1, pp. 1445-1453, 2022.

[14] X. Wang, Z. Wang, Z. Xu, M. Cheng, and Y. Hu, "Optimization of Torque Tracking Performance for Direct-Torque-Controlled PMSM Drives With Composite Torque Regulator," *IEEE Trans on Ind. Electron.*, vol. 67, no. 12, pp. 10095-10108, 2020.

[15] X. Sun, J. Wu, G. Lei, Y. Guo, and J. Zhu, "Torque Ripple Reduction of SRM Drive Using Improved Direct Torque Control With Sliding Mode Controller and Observer," *IEEE Trans on Ind. Electron.*, vol. 68, no. 10, pp. 9334-9345, 2021.

[16] H. Hadla and F. Santos, "Performance Comparison of Field-oriented Control, Direct Torque Control, and Model-predictive Control for SynRMs," *Chinese J. of Electrical Engineering*, vol. 8, no. 1, pp. 24-37, 2022.

[17] Z. Yassine, A. Mohamed, F. Chaymae, and G. Sara, "Induction Motor DTC Performance Improvement by Reducing Flux and Torque Ripples in Low Speed," *Journal of Robotics and Control*, vol. 3, no. 1, 2022.

[18] I. M. Mehedi, N. Saad, M. A. Magzoub, U. M. Al-Saggaf, and A. H. Milyani, "Simulation Analysis and Experimental Evaluation of Improved Field-Oriented Controlled Induction Motors Incorporating Intelligent Controllers," *IEEE Access*, vol. 10, pp. 18380-18394, 2022.

[19] A. Patil and S. Jadhav, "Fuzzy Logic Controller Implementation for BLDC Drive Speed Control Using FOC Approach and SVPWM Based VSI Technique," *2023 Asian Conference on Innovation in Technol*., pp. 1-5, 2023.

[20] A. Devanshu, M. Singh, and N. Kumar, "An Improved Nonlinear Flux Observer Based Sensorless FOC IM Drive With Adaptive Predictive Current Control," *IEEE Trans on Power Electron*., vol. 35, no. 1, pp. 652-666, 2020.

[21] S. Khadar, H. Abu-Rub, and A. Kouzou, "Sensorless Field-Oriented Control for Open-End Winding Five-Phase Induction Motor With Parameters Estimation," *IEEE Open J. of the Ind. Electron. Society*, vol. 2, pp. 266-279, 2021.

[22] G. K. Alitasb, "Integer PI, fractional PI and fractional PI data trained ANFIS speed controllers for indirect field oriented control of induction motor," *Heliyon*, vol. 10, no. 18, 2024.

[23] A. Devanshu, M. Singh, and N. Kumar, "An Improved Nonlinear Flux Observer Based Sensorless FOC IM Drive With Adaptive Predictive Current Control," *IEEE Trans. on Power Electron.*, vol. 35, no. 1, pp. 652-666, 2020.

[24] A. Najem, A. Moutabir, A. Ouchatti, and M. El Haissouf, "Experimental Validation of the Generation of Direct and Quadratic Reference Currents by Combining the Ant Colony Optimization Algorithm and Sliding Mode Control in PMSM using the Process PIL," *International Journal of Robotics & Control Systems*, vol. 4, no. 1, 2024.

[25] F. Shiravani, P. Alkorta, J. A. Cortajarena, and O. Barambones, "An enhanced sliding mode speed control for induction motor drives," in *Actuators*, vol. 11, no. 1, p. 18, 2022.

[26] Y. Zahraoui, M. Moutchou, S. Tayane, C. Fahassa, and S. Elbadaoui, "Induction Motor Performance Improvement using Super Twisting SMC and Twelve Sector DTC," *International Journal of Robotics and Control Systems*, vol. 4, no. 1, pp. 50-68, 2024.

[27] C. Lascu, A. Argeseanu, and F. Blaabjerg, "Supertwisting Sliding-Mode Direct Torque and Flux Control of Induction Machine Drives," *IEEE Trans. on Power Electron.*, vol. 35, no. 5, pp. 057-065, 2020.

[28] A. Nurettin and N. İnanç, "High-Performance Induction Motor Speed Control Using a Robust Hybrid Controller With a Supertwisting Sliding Mode Load Disturbance Observer," *IEEE Trans. on Ind. Electron.*, vol. 70, no. 8, pp. 7743-7752, 2023.

[29] D. Zellouma, H. Benbouhenni, and Y. Bekakra, "Backstepping Control Based on a Third-order Sliding Mode Controller to Regulate the Torque and Flux of Asynchronous Motor Drive," *P.P. Electrical Eng and Computer Science*, vol. 67, no. 1, pp. 10–20, 2023.

[30] N. T. Pham, "Speed Tracking of Field Oriented Control SPIM Drive using (BS_SOSM) Nonlinear Control Structure," *WSEAS Trans on Systs and Cont.*, vol. 14, pp. 291-299, 2019.

[31] J. E. Ruiz-Duarte and A. G. Loukianov, "Sliding mode output-feedback causal output tracking for a class of discrete-time nonlinear systems," *Int. J. of Robust and nonlinear control*, vol. 29, no. 6, pp. 1956-1975, 2019.

[32] M. Megrini, A. Gaga, and Y. Mehdaoui, "Enhancement of field oriented control for permanent magnetic synchronous motor using ant colony optimization," *WSEAS Transactions on Power Systems*, vol. 19, pp. 18-25, 2024.

[33] H. Maghfiroh, A. Ma'arif, F. Adriyanto, I. Suwarno, and W. Caesarendra, "Adaptive Linear Quadratic Gaussian Speed Control of Induction Motor Using Fuzzy Logic," *Journal Européen des Systèmes Automatisés*, vol. 56, no. 4, pp. 703-711, 2023.

[34] M. A. Mossa, H. Echeikh, and N. V. Quynh, "A Novel Sensorless Predictive Voltage Control for an Induction Motor Drive Based on a Back-Stepping Observer-Experimental Validation," *IEEE Access*, vol. 9, pp. 11921-11942, 2021.

[35] A. A. Salem, N. A. N. Aldin, A. M. Azmy, and W. S. E. Abdellatif, "Implementation and Validation of an Adaptive Fuzzy Logic Controller for MPPT of PMSG-Based Wind Turbines," *IEEE Access*, vol. 9, pp. 165690-165707, 2021.

[36] W. Qiu, X. Zhao, A. Tyrrell, S. Perinpanayagam, S. Niu, and G. Wen, "Application of Artificial Intelligence-Based Technique in Electric Motors: A Review," *IEEE Trans. on Power Electron*., vol. 39, no. 10, pp. 543-568, 2024.

[37] B. Farid, B. Tarek, and B. Sebti, "Fuzzy super twisting algorithm dual direct torque control of doubly fed induction machine," *Int. J. of Electrical and Comput. Engineering*, vol. 11, no. 5, pp. 3782-3790, 2021.

[38] N. Farah *et al*., "Investigation of the Computational Burden Effects of Self-Tuning Fuzzy Logic Speed Controller of Induction Motor Drives With Different Rules Sizes," *IEEE Access*, vol. 9, pp. 155443-155456, 2021.

[39] R. A. K. Aswad, B. M. H. Jassim, B. Zahawi, and S. Gadoue, "Hybrid Model-Based Fuzzy Logic Diagnostic System for Stator Faults in Three-Phase Cage Induction Motors," *IEEE Access*, vol. 11, pp. 75707-75714, 2023.

[40] P. Chotikunnan *et al*., "Comparative Study of Takagi-Sugeno-Kang and Madani Algorithms in Type-1 and Interval Type-2 Fuzzy Control for Self-Balancing Wheelchairs," *International Journal of Robotics and Control Systems*, vol. 3, no. 4, pp. 643-657, 2023.

[41] S. Malo and R. Griñó, "Adaptive feed-forward cancellation control of a full-bridge DC-AC voltage inverter," *IFAC Proceedings*, vol. 41, no. 2, pp. 4571–4576. 2008.

[42] L. Rosca and M. Duguleana, "An online observer for minimization of pulsating torque in SMPM motors," *PloS One*, vol. 11, no. 4, 2016.

[43] T. H. Yan, B. He, X. D. Chen, and X. S. Xu, "The discrete-time sliding mode control with computation time delay for repeatable run-out compensation of hard disk drives," *Mathematical Problems in Engineering*, vol. 2, pp. 1–13, 2013.

[44] C. Zhong, Z. Chen, and Y. Guo, "Attitude control for flexible spacecraft with disturbance rejection," *IEEE Trans. on Aerospace and Electron. Syst*., vol. 53, no. 1, pp. 101–110, 2017.

[45] H. Xie, Y. Zhang, K. Song, and C. Shao, "Disturbance Rejection based Engine Speed Control with Rotational Inertia Online Estimation," *2021 40th Chinese Control Conference (CCC)*, 2021.

[46] E. Shahmoradi and M. Mojiri, "Rejection of Sinusoidal Disturbance of Unknown Frequency in Linear Systems with Unknown Input Delay," *Int. Conference on Control, Instrumentation and Automation (ICCIA)*, pp. 1-6, 2023.

[47] T. -B. Airimitoaie, I. D. Landau, R. Melendez, and L. Dugard, "Algorithms for Adaptive Feedforward Noise Attenuation—A Unified Approach and Experimental Evaluation," *IEEE Trans. on Control Syst. Tech.*, vol. 29, no. 5, pp. 1850-1862, 2021.

[48] J. Stewart and P. Ioannou, "Rejection of Sinusoidal Disturbances With Unknown Slowly Time-Varying Frequencies for Linear Time-Invariant Systems," *IEEE Trans. on Auto. Control*, vol. 69, no. 8, pp. 5531-5537, 2024.

[49] N. Abou-Qamar and C. Hatziadoniu, “Cancellation of harmonic torque disturbance in permanent magnet synchronous motor drives by using an adaptive feedforward controller,” *IET Power Electron*., vol. 11, no. 14, pp. 2215-2221, 2018.

[50] R. I. Alfian, A. Ma’arif, and S. Sunardi, “Noise Reduction in the Accelerometer and Gyroscope Sensor with the Kalman Filter Algorithm Rio,” *Journal of Robotics and Control*, vol. 2, no. 3, pp. 180-189, 2021.

[51] Y. Yan, J. Yang, Z. Sun, C. Zhang, S. Li, and H. Yu, "Robust Speed Regulation for PMSM Servo System With Multiple Sources of Disturbances via an Augmented Disturbance Observer," in *IEEE/ASME Transactions on Mechatronics*, vol. 23, no. 2, pp. 769-780, 2018.

[52] M. R. Stankovic, R. Madonski, S. Shao, and D. Mikluc, “On dealing with harmonic uncertainties in the class of active disturbance rejection controllers,” *I. J. of Control*, vol. 94, no. 10, pp. 1–16, 2020.

[53] Z. Yin, C. Bai, N. Du, C. Du, and J. Liu, "Research on Internal Model Control of Induction Motors Based on Luenberger Disturbance Observer,” *Trans. Ind. Electron.*, vol. 36, no. 7, pp. 8155-8170, 2021.

[54] Y. H. Lan, J. Y. Wu, and J. H. She, “Optimal sliding mode preview repetitive control for continuous-time nonlinear systems,” *International Journal of Control,* vol. 96, no. 10, pp. 2415-2424, 2023.

[55] M. Tian, B. Wang, Y. Yu, Q. Dong, and D. Xu, "Discrete-Time Repetitive Control-Based ADRC for Current Loop Disturbances Suppression of PMSM Drives," *IEEE Trans on Ind Inf*., vol. 18, no. 5, pp. 3138-3149, 2022.

[56] Q. Zhang, H. Guo, Y. Liu, C. Guo, and J. Sun, “Robust plugin repetitive control for speed smoothness of cascaded-PI PMSM drive,” *Mechanical Syst. and Signal Processing*, vol. 163, no. 8, 2021.

[57] M. Zhu, Y. Ye, Y. Xiong, and Q. Zhao, “Parameter robustness improvement for repetitive control in grid tied inverters using IIR filter,” *IEEE Trans. on Power Electron.*, vol. 36, no. 7, pp. 8454–8463, 2021.

[58] D. Khadija, M. Anis, and B. A. Ridha, “A discrete repetitive sliding mode multicontrol for non-linear systems,” *International Journal of Systems Science*, vol. 52, no. 9, pp. 1761-1779, 2021.

[59] N. Derbel, J. Ghommam, and Q. Zhu, “Applications of sliding mode control,” *Springer Singapore*, vol. 79, pp. 335-337, 2017.

[60] Y. Shtessel, C. Edwards, L. Fridman, and A. Levant. *Sliding mode control and observation*. New York: Springer New York, 2014.